QCD CORRECTIONS TO VECTOR BOSON PAIR PRODUCTION VIA WEAK BOSON FUSION*

Barbara Jäger[a], Carlo Oleari[b], Dieter Zeppenfeld[a]

[a]Institut für Theoretische Physik, Universität Karlsruhe
P.O. Box 6980, 76128 Karlsruhe, Germany

[b]Dipartimento di Fisica "G. Occhialini", Università di Milano-Bicocca
20126 Milano, Italy

(Received November 15, 2007)

NLO–QCD corrections to vector boson pair production via weak boson fusion have recently been calculated and implemented into flexible parton-level Monte Carlo programs. These allow for the computation of cross sections and kinematical distributions within realistic experimental cuts. We summarize the basic elements of the calculation and review phenomenological results for the LHC.

PACS numbers: 14.70.Hp, 14.80.Bn

1. Introduction

One of the major goals of the CERN Large Hadron Collider (LHC) is the understanding of the mechanism of electroweak (EW) symmetry breaking [1]. In this context, vector–boson fusion (VBF) processes form a promising class of reactions: Higgs production in VBF, *i.e.* the reaction $qq \to qqH$, has been proposed as a particularly clean channel for the discovery of the Higgs boson and a later determination of its couplings [2]. An important background to the $H \to VV$ decay channel ($V = W$ or Z) in VBF is constituted by continuum VV production via VBF, *i.e.* EW $pp \to VVjj$ production [3]. The precise knowledge of the standard model cross section for this reaction at NLO–QCD accuracy becomes crucial for distinguishing enhancements in VBF processes due to signatures of new physics, such as strong electroweak symmetry breaking [4], from possible effects of higher order perturbative corrections.

* Presented by Barbara Jäger at the "Physics at LHC" Conference, Kraków, Poland, July 3–8, 2006.

We have, therefore, calculated the NLO–QCD corrections to the reactions $pp \to e^+\nu_e\mu^-\bar{\nu}_\mu jj$ [5], $pp \to e^+e^-\,\mu^+\mu^- jj$, and $pp \to e^+e^-\,\nu_\mu\bar{\nu}_\mu jj$ [6]. In the following we will refer to these processes briefly as "EW $VVjj$ production". Our calculations have been turned into fully flexible parton-level Monte Carlo programs allowing for the computation of cross sections and distributions within realistic experimental cuts, in complete analogy to the similar programs for the Hjj signal [7] and Vjj production [8] via VBF. In this contribution we briefly recollect the elements of our calculation and discuss the basic features of our results.

2. Elements of the calculation

The computation of partonic matrix elements for EW $VVjj$ production is based on the amplitude techniques of Ref. [9]. Special emphasis is put on the development of a numerically stable and fast code. That is achieved by organizing the calculation of the matrix elements in a modular way such that building blocks that are encountered in several diagrams are evaluated only once per phase space point, as described in some detail in Refs. [5, 6]. This feature becomes particularly important for the computation of the real emission corrections to $VVjj$ production due to the large number of contributing diagrams.

Singularities emerging from soft and collinear configurations are regularized in the dimensional-reduction scheme [10] with space-time dimension $d = 4-2\varepsilon$. The cancellation of the divergences with the respective poles from the virtual contributions is performed by introducing the counter-terms of the dipole subtraction method [11]. The analytical form of the phase-space integrated subtraction terms, obtained after the factorization of the parton distribution functions, is given by

$$\langle \mathcal{I}(\varepsilon)\rangle = |\mathcal{M}_{\rm B}|^2\,\frac{\alpha_{\rm s}(\mu_{\rm R})}{2\pi}C_{\rm F}\left(\frac{4\pi\mu_{\rm R}^2}{Q^2}\right)^{\varepsilon}\Gamma(1+\varepsilon)\left[\frac{2}{\varepsilon^2}+\frac{3}{\varepsilon}+9-\frac{4}{3}\pi^2\right]\,, \quad (2.1)$$

in the notation of Ref. [11], with $\mathcal{M}_{\rm B}$ denoting the amplitude of the corresponding Born process and Q^2 the momentum transfer between the initial and final state quark in Fig. 1. The computation of the virtual corrections requires the evaluation of self-energy, triangle-, box-, and pentagon contributions on either the upper or the lower quark line, as sketched in Fig. 1 (b) for one representative diagram. Contributions from graphs with gluons attached to both the upper and lower quark lines vanish at order $\alpha_{\rm s}$. Putting all virtual contributions together, we find

$$\begin{aligned} 2{\rm Re}[\mathcal{M}_V\mathcal{M}_{\rm B}^*] \;=\; & |\mathcal{M}_{\rm B}|^2\frac{\alpha_{\rm s}(\mu_{\rm R})}{2\pi}C_{\rm F}\left(\frac{4\pi\mu_{\rm R}^2}{Q^2}\right)^{\varepsilon}\Gamma(1+\varepsilon) \\ & \times\left[-\frac{2}{\varepsilon^2}-\frac{3}{\varepsilon}+c_{\rm virt}\right] + 2{\rm Re}[\widetilde{\mathcal{M}}_V\mathcal{M}_{\rm B}^*]\,, \end{aligned} \quad (2.2)$$

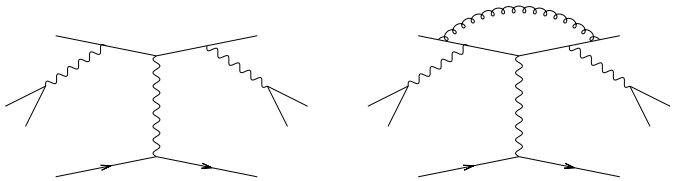

Fig. 1. Representative diagrams contributing to the LO cross section for the process $qq \to qq\,\ell^+\ell^-\ell'^+\ell'^-$ (a) and to the virtual corrections for the same reaction (b).

with $c_{\rm virt} = \pi^2/3 - 7$, and a completely finite remainder $\widetilde{\mathcal{M}}_V$. The divergent pieces in this expression exactly cancel the poles of the counter-terms in Eq. (2.1). The remaining integrals are finite and can be computed numerically in $d = 4$ dimensions by means of a Passarino–Veltman tensor reduction [12]. Numerical stability is achieved by the repeated use of Ward identities which allow us to express a large fraction of the pentagon contributions by a combination of box-type diagrams.

3. Predictions for the LHC

The cross-section contributions discussed above are implemented in fully flexible parton level Monte Carlo programs which allow us to calculate cross sections and kinematical distributions for EW $WWjj$ and $ZZjj$ production at NLO–QCD accuracy within typical experimental acceptance cuts. We use the CTEQ6M parton distributions with $\alpha_{\rm s}(m_Z) = 0.118$ at NLO, and the CTEQ6L1 set at LO [13]. We chose $m_Z = 91.188\,\text{GeV}$, $m_W = 80.419\,\text{GeV}$ and $G_{\rm F} = 1.166 \times 10^{-5}/\,\text{GeV}^2$ as electroweak input parameters, from which we obtain $\alpha_{\rm QED} = 1/132.54$ and $\sin^2\theta_W = 0.22217$. Jets are reconstructed from final-state partons employing the $k_{\rm T}$ algorithm [14, 15] with resolution parameter $D = 0.8$. Throughout, we set fermion masses to zero and neglect external b- and t-quark contributions.

In the following, we consider EW $ZZjj$ production within generic cuts that are relevant for VBF studies at the LHC. We require at least two hard jets with

$$p_{{\rm T}j} \geq 20\ \text{GeV}\,, \qquad\qquad |y_j| \leq 4.5\,, \tag{3.1}$$

where y_j is the rapidity of the (massive) jet momentum which is reconstructed as the four-vector sum of massless partons of pseudorapidity $|\eta| < 5$. The two reconstructed jets of highest transverse momentum are called "tagging jets". To suppress backgrounds to VBF we impose a large rapidity separation of the two tagging jets,

$$\Delta y_{jj} = |y_{j_1} - y_{j_2}| > 4\,. \tag{3.2}$$

In addition, we require the two tagging jets to reside in opposite detector hemispheres,

$$y_{j_1} \times y_{j_2} < 0\,, \tag{3.3}$$

with an invariant mass

$$M_{jj} > 600 \text{ GeV}\,, \tag{3.4}$$

and adopt the lepton cuts

$$\begin{aligned} &p_{\mathrm{T}\ell} \geq 20 \text{ GeV}\,, \qquad |\eta_\ell| \leq 2.5\,, \qquad \triangle R_{j\ell} \geq 0.4\,, \\ &m_{\ell\ell} \geq 15 \text{ GeV}\,, \qquad \triangle R_{\ell\ell} \geq 0.2\,, \end{aligned} \tag{3.5}$$

where $\triangle R_{j\ell}$ and $\triangle R_{\ell\ell}$ denote the jet-lepton and lepton–lepton separation in the rapidity-azimuthal angle plane, respectively, and $m_{\ell\ell}$ the invariant mass of an e^+e^- or $\mu^+\mu^-$ pair.

The total cross section for EW $VVjj$ production contains contributions from the Higgs resonance with $H \to VV$ decays, as well as from VV continuum production. In the following we will focus on the VV continuum by imposing a cut on the four-lepton invariant mass

$$M_{VV} = \sqrt{(p_{\ell_1} + p_{\ell_2} + p_{\ell_3} + p_{\ell_4})^2} > m_H + 10\,\text{GeV}\,, \tag{3.6}$$

where the p_{ℓ_i} denote the four-momenta of the leptons produced in the specific reaction under consideration.

The total continuum cross section for the reaction $pp \to e^+e^-\,\mu^+\mu^-jj$ at NLO within the cuts of Eqs. (3.1)–(3.6) and a Higgs mass of $m_H = 120$ GeV is displayed in Fig. 2 as a function of the renormalization scale $\mu_{\mathrm{R}} = \xi m_Z$ with a fixed factorization scale $\mu_{\mathrm{F}} = m_Z$ (dashed curve), as a function of

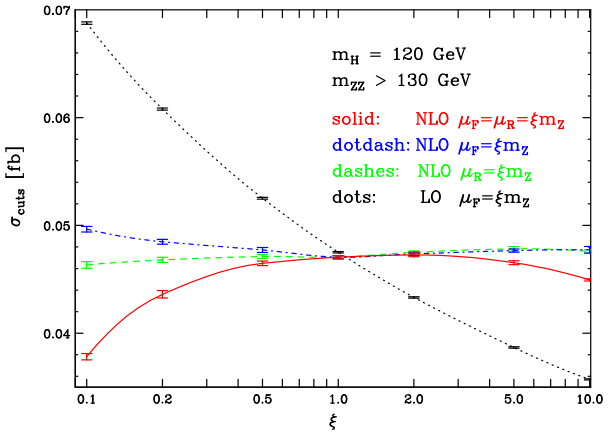

Fig. 2. Dependence of the total $pp \to e^+e^-\,\mu^+\mu^-jj$ continuum cross section at the LHC on the factorization and renormalization scales.

$\mu_{\rm F} = \xi m_Z$ with $\mu_{\rm R} = m_Z$ (dot-dashed curve), and for the case, where both scales are varied simultaneously, $\mu_{\rm R} = \mu_{\rm F} = \xi m_Z$ (solid curve). The LO cross section depends only on $\mu_{\rm F} = \xi m_Z$ (dotted curve). As in the analogous cases of $e^+\nu_e\mu^-\bar{\nu}_\mu$ and $e^+e^-\,\nu_\mu\bar{\nu}_\mu$ production via VBF, discussed in Refs. [5, 6], the scale variations of the NLO prediction are found to be below the 2% level when the scale parameter runs from $\xi = 0.5$ to $\xi = 2.0$, while the LO cross section changes by more than 20% in the same range of ξ.

Fig. 3 shows the transverse momentum distribution of the tagging jet with the highest $p_{\rm T}$ for EW $e^+e^-\,\mu^+\mu^-jj$ production. The factorization and renormalization scales are fixed to $\mu_{\rm F} = \mu_{\rm R} = m_Z$. The K factor, defined by

$$K(x) = \frac{d\sigma_{\rm NLO}/dx}{d\sigma_{\rm LO}/dx} \tag{3.7}$$

and shown for this distribution in Fig. 3 (b), illustrates the change in shape when going from LO to NLO. At NLO, smaller values of $p_{\rm T}$ are preferred by the tagging jet, which is due to the extra parton which emerges in the real emission contributions. In a similar way, other distributions such as the invariant mass distribution of the tagging-jet pair, $d\sigma/dM_{jj}^{\rm tag}$ (see Ref. [6]), or the transverse momentum distributions of the detected leptons are affected by the inclusion of NLO corrections. On the other hand, some angular distributions such as $d\sigma/d\eta_\ell^{\rm max}$, where $\eta_\ell^{\rm max}$ designates the largest lepton rapidity emerging in the scattering, barely change at NLO as illustrated in Fig. 4. The step in $d\sigma/d\eta_\ell^{\rm max}$ at $\eta_\ell^{\rm max} = 2.5$ is due to the rapidity cut imposed on the lepton rapidities in Eq. (3.5).

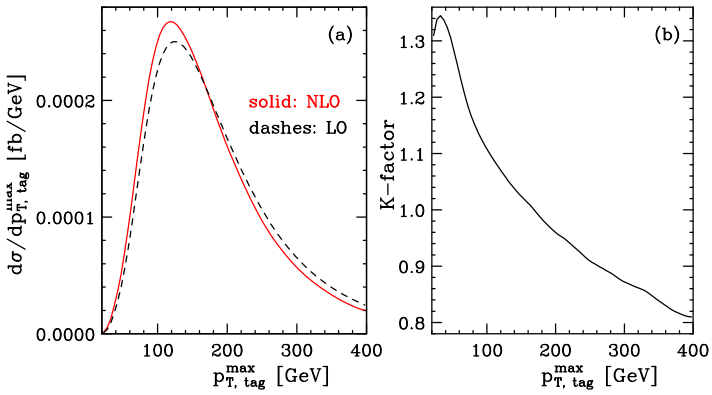

Fig. 3. Transverse momentum distribution of the tagging jet with the highest $p_{\rm T}$ in EW $e^+e^-\,\mu^+\mu^-jj$ production at the LHC. Panel (a) shows the NLO result (solid line) and the LO prediction (dashed line). Panel (b) displays the K factor defined in Eq. (3.7).

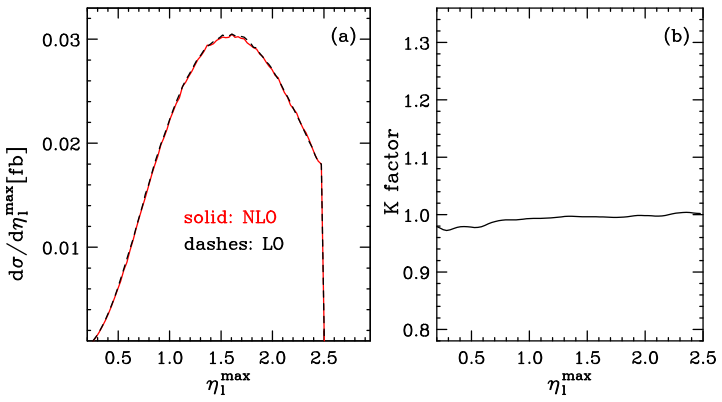

Fig. 4. Distribution of the maximal lepton rapidity in EW $e^+e^-\,\mu^+\mu^-jj$ production at the LHC. Curves are as in Fig. 3.

Our discussion on the effect which higher order QCD corrections have on dynamical K factors has been based on EW $e^+e^-\,\mu^+\mu^-jj$ production. However, the shapes of kinematical distributions in the other VBF production processes we have studied, *i.e.*, $pp \to e^+e^-\,\nu_\mu\bar{\nu}_\mu jj$ and $pp \to e^+\nu_e\mu^-\bar{\nu}_\mu jj$, behave very similarly.

4. Conclusions

In this contribution we have reviewed some results on EW $WWjj$ and $ZZjj$ production at NLO–QCD accuracy obtained with fully flexible Monte Carlo programs. The higher order corrections to these reactions turn out to be under excellent control, as indicated by the small scale dependence of the total cross sections and K factors close to one. We found, however, that some kinematical distributions exhibit a noticeable change in shape when NLO corrections are considered. This indicates the importance of including NLO–QCD contributions in precision studies of VBF processes at the LHC.

This research was supported in part by the Deutsche Forschungsgemeinschaft under SFB TR-9 “Computergestützte Theoretische Teilchenphysik”.

REFERENCES

[1] ATLAS Collaboration, ATLAS TDR, Report No. CERN/LHCC/99-15 (1999); G.L. Bayatian *et al.*, CMS Technical Proposal, Report No. CERN/LHCC/ 94-38x (1994).

[2] D. Zeppenfeld, R. Kinnunen, A. Nikitenko, E. Richter-Was, *Phys. Rev.* **D62**, 013009 (2000) [hep-ph/0002036]; D. Zeppenfeld, Procceedings of the APS/DPF/DPB Summer Study on the Future of Particle Physics, Snowmass, 2001, edited by N. Graf, eConf **C010630**, p. 123 (2001) [hep-ph/0203123]; *J. High Energy Phys.* **0208**, 041 (2002) [hep-ph/0205270]; M. Dührssen *et al., Phys. Rev.* **D70**, 113009 (2004) [hep-ph/0406323].

[3] D. Rainwater, D. Zeppenfeld, *Phys. Rev.* **D60**, 113004 (1999) [hep-ph/9906218], Erratum **D61**, 099901 (2000); N. Kauer, T. Plehn, D. Rainwater, D. Zeppenfeld, *Phys. Lett.* **B503**, 113 (2001) [hep-ph/0012351].

[4] J. Bagger *et al., Phys. Rev.* **D52**, 3878 (1995) [hep-ph/9504426]; M.S. Chanowitz, *Czech. J. Phys.* **55**, B45 (2005) [hep-ph/0412203].

[5] B. Jäger, C. Oleari, D. Zeppenfeld, *J. High Energy Phys.* **0607**, 015 (2006) [hep-ph/0603177].

[6] B. Jäger, C. Oleari, D. Zeppenfeld, *Phys. Rev.* **D73**, 113006 (2006) [hep-ph/0604200].

[7] T. Figy, C. Oleari, D. Zeppenfeld, *Phys. Rev.* **D68**, 073005 (2003) [hep-ph/0306109].

[8] C. Oleari, D. Zeppenfeld, *Phys. Rev.* **D69**, 093004 (2004) [hep-ph/0310156].

[9] K. Hagiwara, D. Zeppenfeld, *Nucl. Phys.* **B274**, 1 (1986); K. Hagiwara, D. Zeppenfeld, *Nucl. Phys.* **B313**, 560 (1989).

[10] W. Siegel, *Phys. Lett.* **B84**, 193 (1979); W. Siegel, *Phys. Lett.* **B94**, 37 (1980).

[11] S. Catani, M.H. Seymour, *Nucl. Phys.* **B485**, 291 (1997), Erratum **B510**, 503 (1997), [hep-ph/9605323].

[12] G. Passarino, M.J. Veltman, *Nucl. Phys.* **B160**, 151 (1979).

[13] J. Pumplin, D.R. Stump, J. Huston, H.L. Lai, P. Nadolsky, W.K. Tung, *J. High Energy Phys.* **0207**, 012 (2002) [hep-ph/0201195].

[14] S. Catani, Yu.L. Dokshitzer, B.R. Webber, *Phys. Lett.* **B285**, 291 (1992); S. Catani, Yu.L. Dokshitzer, M.H. Seymour, B.R. Webber, *Nucl. Phys.* **B406**, 187 (1993); S.D. Ellis, D.E. Soper, *Phys. Rev.* **D48**, 3160 (1993).

[15] G.C. Blazey *et al.*, hep-ex/0005012.